AGU PUBLICATIONS

JGR

Journal of Geophysical Research: Oceans

RESEARCH ARTICLE

10.1002/2015JC010824

Key Points:

- 3-D surge model accurately simulates the vegetation effects
- 2-D surge model with MC approach fails to simulate the vegetation effects
- 3-D model simulates significant onshore sediment transport

Correspondence to:
Email: Y. Peter Sheng,
pete@coastal.ufl.edu

Citation:
Lapetina, A., and Y. P. Sheng (2015), Simulating complex storm surge dynamics: Three-dimensionality, vegetation effect, and onshore sediment transport, *J. Geophys. Res. Oceans*, *120*, 7363–7380, doi:10.1002/2015JC010824.

Received 10 MAR 2015
Accepted 22 SEP 2015
Accepted article online 24 SEP 2015
Published online 16 NOV 2015

Simulating complex storm surge dynamics: Three-dimensionality, vegetation effect, and onshore sediment transport

Andrew Lapetina[1] and Y. Peter Sheng[1]

[1]Coastal and Oceanographic Engineering Program, University of Florida, Gainesville, Florida, USA

Abstract The 3-D hydrodynamics of storm surge events, including the effects of vegetation and impact on onshore transport of marine sediment, have important consequences for coastal communities. Here, complex storm surge dynamics during Hurricane Ike are investigated using a three-dimensional (3-D), vegetation-resolving storm surge-wave model (CH3D-SWAN) which includes such effects of vegetation as profile drag, skin friction, and production, dissipation, and transport of turbulence. This vegetation-resolving 3-D model features a turbulent kinetic energy (TKE) closure model, which uses momentum equations with vegetation-induced profile and skin friction drags, a dynamic q^2 equation including turbulence production and dissipation by vegetation, as well as vegetation-dependent algebraic length-scale equations, and a Smagorinsky-type horizontal turbulence model. This vegetation model has been verified using extensive laboratory tests, but this study is a comparison of 2-D and 3-D simulations of complex storm surge dynamics during Hurricane Ike. We examine the value of 3-D storm surge models relative to 2-D models for simulating coastal currents, effects of vegetation on surge, and sediment transport during storm events. Comparisons are made between results obtained using simple 2-D formulations for bottom friction, the Manning coefficient (MC) approach, and physics-based 3-D vegetation-modeling (VM) approach. Last, the role that the 3-D hydrodynamics on onshore transport and deposition of marine sediments during the storm is investigated. While both the 3-D and 2-D results simulated the water level dynamics, results of the physics-based 3-D VM approach, as compared to the 2-D MC approach, more accurately captures the complex storm surge dynamics.

1. Introduction

Recent catastrophic damage from tropical cyclones such as Superstorm Sandy, Hurricane Ike, and Hurricane Katrina has reminded coastal inhabitants of the importance of a sound scientific understanding of the dynamics of storm surge. Failure to properly capture the mechanics of these complex events can lead to high risks for coastal communities and infrastructure. Consequently, efforts to model the complex 3-D environmental fluid dynamics of storm surge should push scientific boundaries and aim to improve the ability of communities to protect them from coastal hazards. Recent studies have found that vegetated coastal habitats among the most valuable ecosystems on Earth, primarily for their capacities to provide coastal protection, nutrient fluxes, habitat, and CO_2 sinks [*Barbier et al.*, 2011; *Costanza et al.*, 1997; *Duarte et al.*, 2013]. However, empirical methods were used for assessing the flood protection aspect of ecosystem service provided by coastal wetlands. A robust vegetation-resolving surge and wave model is needed to enhance the empirical estimates of the vegetation effects on flooding during real storms as well as future climate scenarios [e.g., *Condon and Sheng*, 2012].

The purpose of this paper is to use simulations of Hurricane Ike to answer pressing questions about complex storm surge dynamics, exploring and articulating the usefulness of 3-D vegetation-and-sediment-resolving models. In this paper, the efficacy of 2-D and 3-D models to capture the 3-D environmental fluid mechanics of storm surge events is compared for an actual large storm event with complex, well-documented hydrodynamic phenomena, including a forerunner [*Kennedy et al.*, 2011], flow through vegetation canopies [*Kerr et al.*, 2013a, 2013b], and marine sediment deposition [*Williams*, 2012]. Three main subtopics of current importance are investigated here using 2-D MC approach and 3-D VM approach: dynamics of coastal currents and water levels during storm, effects of vegetation on storm surge, and onshore sediment transport due to coastal currents during storm.

AQ20

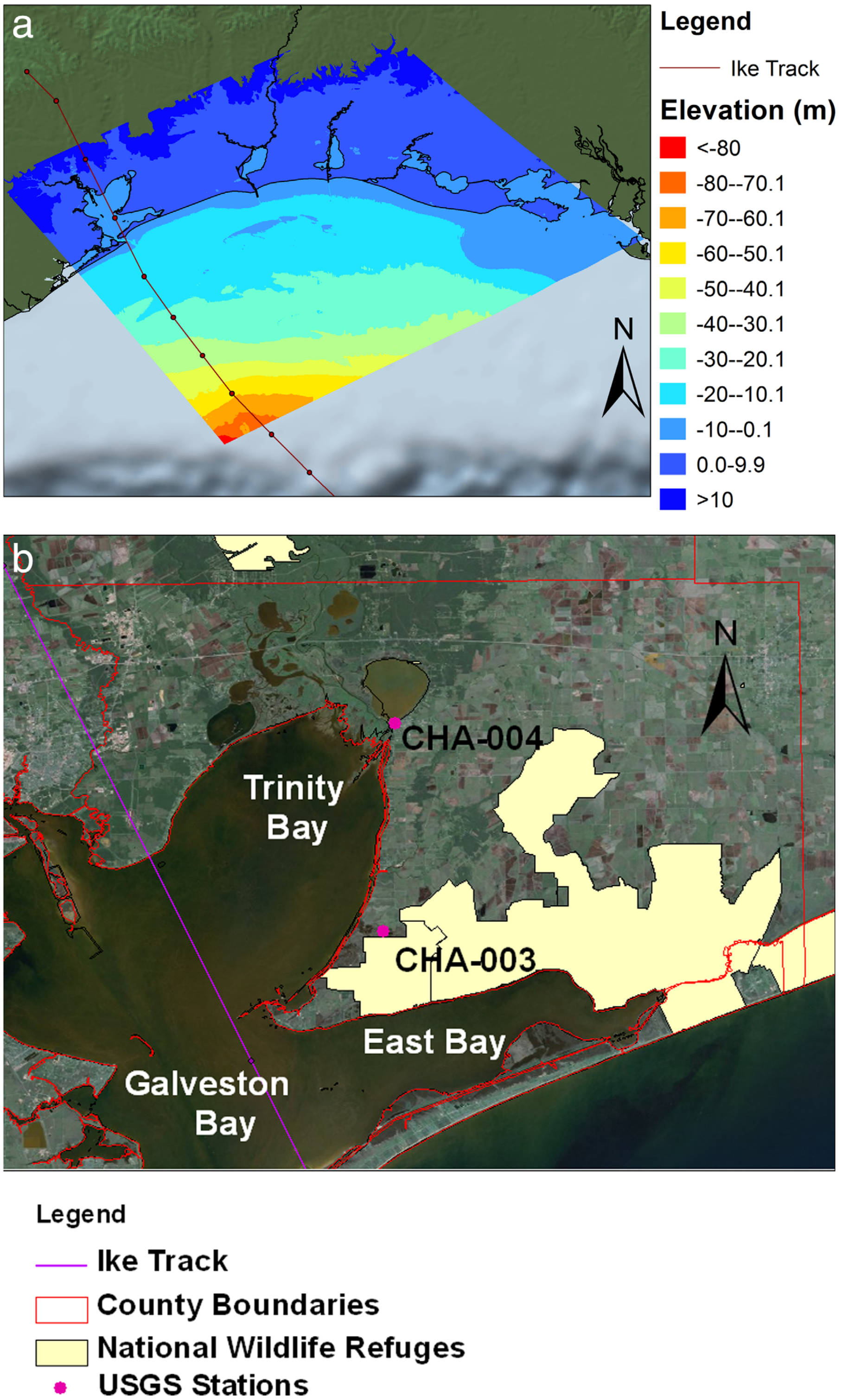

Figure 1. (a) Track for Hurricane Ike, Domain, and (b) area of special interest.

Hurricane Ike made landfall near Galveston, Texas on 13 September 2008 (Figure 1). While the storm was noted for its unusually high storm surge well ahead of landfall [*Kennedy et al*., 2011], it was also a remarkably well-documented storm from an observational perspective [*Tweel and Turner*, 2012; *Williams*, 2012; *Hope et al*., 2013]. Furthermore it has been the subject of many 2-D and two-layer modeling efforts

[*Rego and Li*, 2010; *Kennedy et al*., 2011; *Hope et al*., 2013; *Kerr et al*., 2013a, 2013b]. With so many 2-D modeling efforts of this storm, it represents a good opportunity to compare the efficacy of 2-D and 3-D models. The 3-D model used here is CH3D-SSMS, which has been enhanced to include a vegetation module [*Sheng et al*., 2012] and a sediment transport module [*Sheng and Villaret*, 1989; *Sheng et al*., 2002; *Sheng and Kim*, 2009].

1.1. 2-D Versus 3-D Modeling

Storm surge dynamics are dominated by the interaction of surface winds and bottom friction, though other factors such as wave [*Sheng and Liu*, 2011], Coriolis [*Kennedy et al*., 2011], and baroclinic effects [*Tutak and Sheng*, 2011] can be quite important. Recent efforts to simulate Hurricane Ike have been effective at simulating accurate water levels in 2-D using large, high-resolution computational domains [*Kerr et al*., 2013a, 2013b; *Hope et al*., 2013]. Utilizing a Chezy-Manning bottom friction parameterization [*Gauckler*, 1867*; Manning*, 1891; *Chow*, 1959] with a spatially varying Manning coefficient (MC) which mimics the bottom roughness, these studies produced reasonably accurate hydrographs and maximum water elevations when compared with data from this storm.

Lapetina and Sheng [2014], hereafter referred to as LS14, noted that while enhancing the MC of a 2-D model can produce accurate water levels in 3-D storm surge events, it causes deviations between simulated 2-D (vertically-averaged) and observed or simulated 3-D velocities. This is because 2-D models calculate a single vertically averaged velocity, while 3-D models determine velocities at several vertical locations from the bottom of the water column to the surface. While these 2-D models can produce reasonable water levels and hydrographs, their velocities usually do not match with observation. Moreover, in order to verify the simulated 2-D vertically averaged velocity, it is necessary to obtain the observed vertical profile of horizontal velocities before an accurate vertically averaged velocity can be calculated by proper averaging. To verify a 3-D model, however, observed velocity at any vertical layer can be used for comparison with simulated 3-D velocity. Therefore, verification of the 2-D vertically averaged velocity is more difficult than that for a 3-D model.

LS14 showed that, when vegetation is present, inundation results of 2-D and 3-D models can be made similar for a single storm of constant intensity. This is consistent with the finding of *Weaver and Luettich* [2009]. However, *LS14* showed that 2-D and 3-D simulated flow and inundation results differ considerably for different storms, unless the Manning coefficient is adjusted as the storm intensity changes. Using the same Manning coefficient for all storms (with intensities of 1, 2, 3, 4, and 5) in 2-D simulations, *LS14* found that 2-D and 3-D water levels near the coastal vegetation can differ by 40 cm. This suggests that while changing the Manning coefficient for a single storm of constant intensity may produce good water level results, this is not a reliable way to predict the surge and inundation during a storm of varying intensity. Water velocity during a storm has important impacts in determining forces on offshore structures [*Bode and Hardy*, 1997], transporting pollutants [*Liu and Sheng*, 2014], and modeling complex geophysical processes [*Hope et al*., 2013]. While there is undisputed value in status-quo 2-D storm surge models for forecasting water levels, particularly the highly efficient SLOSH model used by the National Hurricane Center [*Jelesnianski et al*., 1992] as well as the high-resolution ADCIRC model [*Luettich et al*., 1992], questions remain about the ability of 2-D models to accurately capture all of the 3-D physical processes of surge, such as the influence of vegetation and coastal currents [*Bode and Hardy*, 1997; *Resio and Westerink*, 2008; *Weisberg and Zheng*, 2008], flow structures in vegetated flows [*Nepf and Vivoni*, 2000; *Neumeier*, 2007], and onshore sediment transport. While it is possible to parameterize the various 3-D processes related to sediment transport, e.g., wave-current bottom boundary layer and vertical stratification [*Grant and Madsen*, 1979; *Sheng and Villaret*, 1989], vertically varying wave-induced circulation [*Sheng and Liu*, 2011; *Kumar et al*., 2011], and sediment deposition and resuspension [*Sheng*, 1986]; considerable effort is needed to tune the highly parameterized 2-D models to reproduce the vertically averaged results of observed or simulated 3-D sediment transport.

In this paper, 2-D and 3-D simulations are compared to data obtained during Hurricane Ike to explore their differences. Section 2.2 describes model simulations used to compare the two, section 3.1 includes results from these simulations, and section 4.1 contains a discussion of these results.

1.2. The Influence of Vegetation on Storm Surge

The hydrodynamics of wind-driven water flow is complicated for environments such as vegetation-laden coastal wetlands, which are critically important for reducing storm surge near at-risk coastal infrastructure.

In vegetation-laden environments, the vertical structure of wind-driven flow is dependent on many factors, particularly the ratio of water depth H to vegetation height K [*Nepf and Vivoni*, 2000]. Because the water depth, and therefore this ratio, varies significantly over the course of a storm as water levels rise and fall in time, simple parameterizations of bottom friction using a MC cannot accurately capture all of the physical processes within a complex, 3-D, storm surge. *Bode and Hardy* [1997] found that the importance of 3-D models is in their ability to calculate the vertical profile of storm-induced currents, and that 2-D models may have a questionable validity for determining complex dynamics.

Most 2-D models use a constant or variable MC to account for bottom roughness in 2-D flow [*Blumberg*, 1977; *Bunya et al*., 2010; *Kerr et al*., 2013a, 2013b]. On the other hand, 3-D models generally recognize the existence of a thin bottom boundary layer within which the velocity varies logarithmically [see, e.g., *Tennekes and Lumley*, 1972] and uses a roughness height value z_0 based on the physical conditions of the bottom sediments, and model velocities at discrete locations between the ocean bottom and water surface [e.g., *Sheng et al*., 2010a, 2010b]. Likewise, attempts to model the effects of vegetation on storm surge have relied on both 2-D and 3-D models [see, e.g., *Ferreiera, et al*., 2014]. 2-D models increase the MC for bottom friction to represent all of the frictional effects of vegetation [*Liu et al*., 2013; *Zhang et al*., 2012], including profile drag, shear friction drag, and Reynolds stresses throughout the water column. *Liu et al*. [2013] studied the effects of mangroves on reducing storm surge and flooding in southern Florida by changing the MC in their 2-D model. In their model, the drag of vegetation stems acting on the flow is treated as a bottom friction and may cause an overestimation of bottom shear stress that is used to suspend sediments from bed in the modeling of sediment transport [*Hu et al*., 2015].

3-D representations of vegetation [*Sheng et al*., 2012; LS14] use a turbulent kinetic energy (TKE) closure model to include all the effects of vegetation in 3-D, incorporating the vegetation-induced profile drag, skin friction, turbulence dissipation, and TKE production throughout the water column. *Sheng et al*. [2012] quantitatively assessed the flood protection capacity of coastal wetlands (with various widths, heights, and densities) during hurricanes (of various intensities and forward speeds) in terms of the Vegetation Dissipation Potential (VDP), which is the percent reduction of total inundation volume (TIV) due to the presence of vegetation canopy. *Hu et al*. [2015] used a similar measure to assess the dissipation of surge by coastal wetlands in Louisiana during Isaac. *Hortsman et al*. [2013] simulated tidal dynamics in a mangrove creek catchment using 2-D and 3-D models. In this study, for the first time, a 3-D model is used along with a 2-D model to simulate the comprehensive effects of vegetation on storm surge during Hurricane Ike. This represents a step forward in understanding complex surge dynamics as well as a scientific advancement in storm surge modeling [*Resio and Westerink*, 2008].

LS14 compared the ability of 2-D and 3-D storm surge models to accurately simulate the influence of vegetation on storm surge through a two-part study on an idealized domain. First, they ran 2-D and 3-D simulations for a Category 2 storm on a coastal region with a simple gentle-sloped shelf. These 2-D and 3-D simulations, representing the vegetation using an empirically enhanced MC and a vegetation-resolving vertically varying TKE model, respectively, produced very similar inundation patterns and water levels by tuning the MC of the 2-D model. Then, they used these same domains and 2-D and 3-D vegetation representations to model Category 1 through Category 5 storms, and found that the Category 1 and Category 3–5 storms produced very different inundation patterns for 2-D and 3-D representations of vegetation. In summary, the 2-D (enhanced MC) model and 3-D (VM) model of vegetation were capable of producing the same water levels for a Category 2 storm but, because their differences in modeling of storm surge dynamics, they are incapable of producing similar water levels for multiple storms of different intensities and other properties. Essentially, the results revealed that the MC in the 2-D model is a function of the flow (which varies with the hurricane) as well as the vegetation condition, hence the MC will have to be adjusted from one storm to another. This finding is consistent with the findings of ADCIRC simulations. For example, MC used by the ADCIRC model for Ike [*Hope et al*., 2013] is about 50% of that used for Katrina [*Bunya et al*., 2010].

In this paper, for the first time, the ability of 2-D (MC) and 3-D (VM) models of vegetation to simulate the effects of vegetation on storm surge dynamics will be compared for a real storm. 2-D and 3-D simulations of Hurricane Ike, including tides, winds, waves, Coriolis effects, bottom friction, and vegetation effects are described in section 2.3, with results shown in section 3.2. In section 4.2, a comparison of the two representations is made.

1.3. Sediment Dynamics

Recent research has explored the deposition of marine sediment on coastal wetlands due to hurricanes [*Turner et al*., 2006; *Williams*, 2012; *Tweel and Turner*, 2012], and found that hurricanes play an important role in bringing marine sediment onshore to build land, rather than eroding it. Many of these papers concluded that improved modeling of nearshore hydrodynamics associated with storm events can improve understanding of sediment transport in storms, as well as paleotempestology, long-term geomorphology, and wetland dynamics.

However, little modeling study of sediment transport in storms has actually been conducted by storm surge modelers, though sediment transport in storms has been identified as an area of great concern [*Resio and Westerink*, 2008]. Here, 3-D simulations which include sediment transport and Coriolis (Ekman layer) effects are compared to results from 2-D simulations of Hurricane Ike to explore their differences. However, it should be noted that this study does not include a detailed investigation of the morphodynamics which requires very high horizontal grid resolution (~1–5 m) modeling and observation which is largely unavailable. A 2-D sediment transport modeling is not conducted here because of the fundamental 3-D nature of the sediment transport processes including wave-induced circulation, wave-current bottom boundary layer, vertical sediment stratification, and deposition and resuspension, as pointed out earlier in the paper. Although it is possible to parameterize all the above 3-D processes, it is unlikely that 2-D model will produce results better than the 3-D results, particularly when little data exists to tune the 2-D model parameters. Section 2.4 describes sediment transport model and sediment transport simulations, section 3.3 includes results from these simulations, and section 4.3 contains a discussion of these results.

2. Methods

2.1. Model Setup and Inputs

All model simulations included in this paper contain some common inputs and hydrodynamic equations. This paper utilizes a fully 3-D, coupled storm-surge and wave model. CH3D-SSMS (Curvilinear Hydrodynamics in 3D—Storm Surge Modeling System), has been used to simulate hurricanes Isabel [*Sheng et al*., 2010a], Ivan [*Sheng et al*., 2010b], Charley [*Davis et al*., 2010], Wilma [*Condon et al*., 2013], and many other storms. The hydrodynamics of CH3D-SSMS are determined by a coupled CH3D-SWAN circulation-wave model. Detailed curvilinear equations for CH3D, including radiation stress, bottom friction formulation, and wave bottom boundary effects can be found in *Sheng et al*. [2010a]. Equations for SWAN can be found in *Booij et al*. [1999].

CH3D-SSMS uses the hydrostatic and Boussinesq approximations, eddy viscosity closure, and assumes incompressibility. It can be run in 2-D mode as well as 3-D mode, which allows easy comparison of 2-D and 3-D results. CH3D-SSMS operates on a terrain-following sigma grid in the vertical direction and a boundary-fitted non-orthogonal curvilinear grid in the horizontal directions, shown in Figure 1. The model domain contains 1472-by-1408 cells, and stretches from Marsh Island to halfway down Galveston Island, and 3-D simulations had four or eight layers. The average horizontal grid resolution is 190 m × 190 m, while the smallest grid size is 30 m × 30 m, near Galveston Inlet. Bathymetry of the grid was based on data acquired from NOAA's NGDC Coastal Relief Model (http://www.ngdc.noaa.gov/mgg/coastal/startcrm.htm).

Winds were acquired from the H*Wind database from the Atlantic Oceanographic and Meteorological Laboratory [*Powell et al*., 1998]. Snapshots of 3 hourly data were temporally and spatially interpolated onto the domain, and comparisons to data collected at various airports show fairly good agreement. No background winds were superimposed.

3-D simulations are conducted with a 1s time step, while 2-D simulations are conducted with a 10 s time step unless otherwise noted. The CH3D-SSMS requires boundary conditions for both CH3D and SWAN. Tidal effects were included by using the ADCIRC tidal database [ADCIRC Tidal Database, version ed_95d; see http://www.unc.edu/ims/ccats/tides/tides.htm]. Tidal constituents include M2, N2, K1, S2, O1, K2, and Q1. Tidal simulations confirmed a bottom roughness length Z_o of 0.05 cm and a MC of 0.017. Water level associated with surge at the boundary was provided by the HYCOM database [www.hycom.org, accessed May 2012]. Wave conditions such as significant wave height, average period, and direction were provided by Wave Watch III [polar.ncep.noaa.gov/waves, accessed May 2012].

Wave coupling for CH3D-SSMS is through dynamic two-way coupling between CH3D and SWAN [*Booij et al*., 1999] which is a third generation wave model. SWAN receives wind, current, and water level data

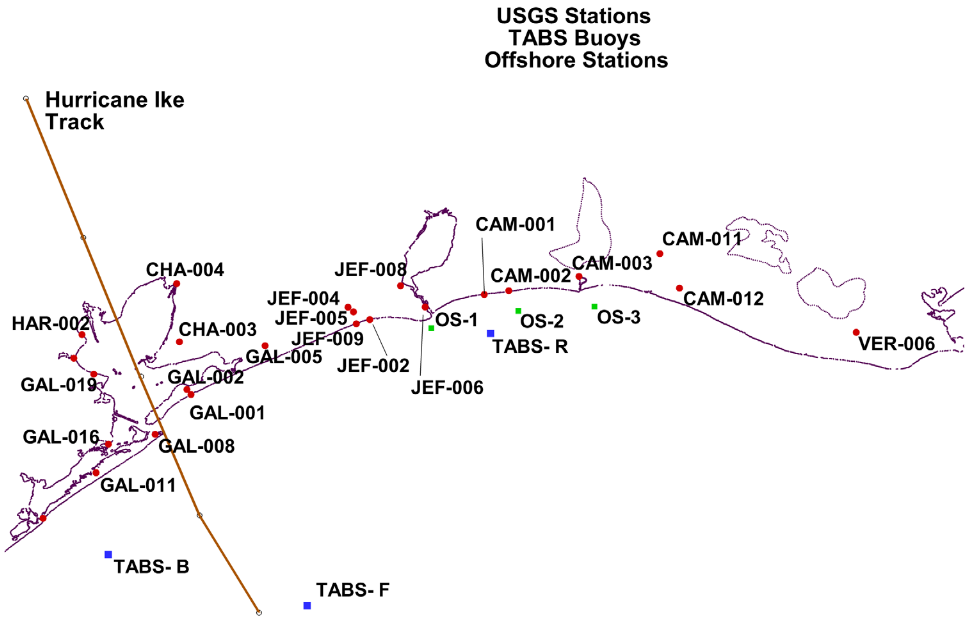

Figure 2. Stations used for comparisons of different model features.

from CH3D, and then sends data on significant wave height, peak period, and wave direction back to CH3D. This is done every 30 min of simulation time, in a fashion similar to *Sheng et al.* [2010a]. Wave boundary conditions were acquired from the WAVEWATCH III archives.

2.2. 2-D Versus 3-D Comparisons

To enable timely response and evacuation actions during hurricanes, there is a need for expedient and accurate 2-D and 3-D model simulations of storm surge. Here 2-D and 3-D model simulations are conducted and their results compared in detail to evaluate the efficacy of these two approaches. Simulations are all 4 days long, and contain the same wind and wave forcing. However, 2-D simulations contain a MC bottom friction formulation, and calculate a single vertically averaged velocity at every location, while 3-D vegetation-free simulations contain a quadratic bottom friction formulation representing the existence of a logarithmic bottom boundary layer, and determine velocities at four or eight vertical locations between the ocean bottom and water surface. Results obtained with four and eight vertical layers show negligible difference. Consequently, the hydrodynamic complexity of 3-D simulations is greater, permitting calculation of turbulent boundary layers, Reynolds stresses, and vertically varying velocities.

Time series of water levels over the entire model domain are available from the USGS [http://pubs.usgs.gov/of/2008/1365/, accessed May 2012]. This mobile network of gauges collected data at 56 sites in Louisiana and Texas in beaches, estuaries, wetlands, and river mouths. All sites were temporally synced and tied to the NAVD 88 datum, providing a very high-quality water level data set. To compare this water level data to model results, each data set was temporally averaged every 10 min, to smooth results.

In addition, comparisons are made here for 2-D and 3-D water velocities versus observed velocities during Hurricane Ike at three offshore buoys operated by the Texas Automated Buoy System (TABS). Locations for TABS Buoys and USGS water level meters are shown in Figure 2. 2-D velocities are highly dependent upon the MC used [*Kerr et al*., 2013a, 2013b]. Therefore, 2-D simulations are conducted with various MC on the open ocean, and their velocities are compared to the vertically averaged, surface, and near-bottom velocities obtained in a 3-D simulation. Two different open ocean MC's are used, 0.01, which was required by ADCIRC to simulate Hurricane Ike [*Hope et al*., 2013], and 0.017, a value closer to the canonical MC used to simulate open ocean roughness in many other ADCIRC simulations [e.g., *Bunya et al*., 2010; *Wamsley et al*., 2010]. The simulations used for this comparison are described in Table 1. Simulations D1 and D3 used spatially uniform MC, while simulation D2 used the MC map used by ADCIRC as described in section 2.3, and shown in Figure 3a. Results for these three simulations are given in section 3.1.

Table 1. Simulations Conducted to Compare the Importance of Dimensionality and Velocity

Model Simulation #	Model Dimensionality	Z_0 (3D) or MC (2D) in the Open Ocean
D1	3D	0.05 cm
D2	2D	0.01
D3	2D	0.017

2.3. Comparison of Vegetation Representations: MC Versus VM

Representing vegetation in a 2-D model is primarily done by empirically enhancing the MC [*Ferriera, et al.*, 2014], while *LS14* showed that a vegetation-resolving TKE model, i.e., a vegetation model (VM), can be used to include the effects of vegetation on flow and turbulence in 3-D. These two methods for modeling the influence of vegetation on storm surge will be compared with observation during Hurricane Ike.

While the 2-D MC approach is well-documented [*Loder et al.*, 2009; *Liu et al.*, 2013; *Lapetina and Sheng*, 2014; *Hope et al.*, 2013], the TKE model for vegetation, or VM, [*Sheng et al.*, 2012; *Lapetina and Sheng*, 2014] requires some description here. When vegetation is present, the *u, v* and *w* momentum equations, including the effects of vegetation but ignoring baroclinic effects in Cartesian and z coordinates are:

$$\begin{aligned}&\frac{\partial u}{\partial t}+\frac{\partial uu}{\partial x}+\frac{\partial uv}{\partial y}+\frac{\partial uw}{\partial z}+\frac{1}{\rho_w}\frac{\partial S_{xx}}{\partial x}+\frac{1}{\rho_w}\frac{\partial S_{xy}}{\partial y}\\&=-\left[C_fA_w+C_pA_f\left(1+\frac{u^2}{q^2}\right)^{1/2}\right]qu-g\frac{\partial \eta}{\partial x}-\frac{1}{\rho_w}\frac{\partial P}{\partial x}+fv+A_H\left(\frac{\partial^2 u}{\partial x}+\frac{\partial^2 u}{\partial y}\right)+\frac{\partial}{\partial z}\left(A_v\frac{\partial u}{\partial z}\right)\end{aligned} \tag{1}$$

$$\begin{aligned}&\frac{\partial v}{\partial t}+\frac{\partial uv}{\partial x}+\frac{\partial vv}{\partial y}+\frac{\partial vw}{\partial z}+\frac{1}{\rho_w}\frac{\partial S_{yx}}{\partial x}+\frac{1}{\rho_w}\frac{\partial S_{yy}}{\partial y}\\&=-\left[C_fA_w+C_pA_f\left(1+\frac{v^2}{q^2}\right)^{1/2}\right]qv-g\frac{\partial \eta}{\partial y}-\frac{1}{\rho_w}\frac{\partial P}{\partial y}-fu+A_H\left(\frac{\partial^2 v}{\partial x}+\frac{\partial^2 v}{\partial y}\right)+\frac{\partial}{\partial z}\left(A_v\frac{\partial v}{\partial z}\right)\end{aligned} \tag{2}$$

$$\rho g=-\frac{\partial p}{\partial z} \tag{3}$$

where *x*, *y*, and *z* are three spatial dimensions; *t* is time; *u*, *v*, and *w* are velocities in three dimensions; ρ_w is water density, constant here; S_{xx}, S_{xy}, S_{yy} are radiation stresses; *g* is gravity; η is water level; *P* is atmospheric pressure; *p* is the hydrostatic pressure; *f* is the Coriolis parameter; A_H is the *Smagorinsky* [1964] type horizontal eddy viscosity which varies with the local flow and grid spacing; and A_v is the vertical eddy viscosity. A complete description of these terms, and conversion of these equations to curvilinear and sigma coordinates is available from *Sheng et al.* [2010a]. An additional equation, the continuity equation, is shown below:

$$\frac{\partial u}{\partial x}+\frac{\partial v}{\partial y}+\frac{\partial w}{\partial z}=0 \tag{4}$$

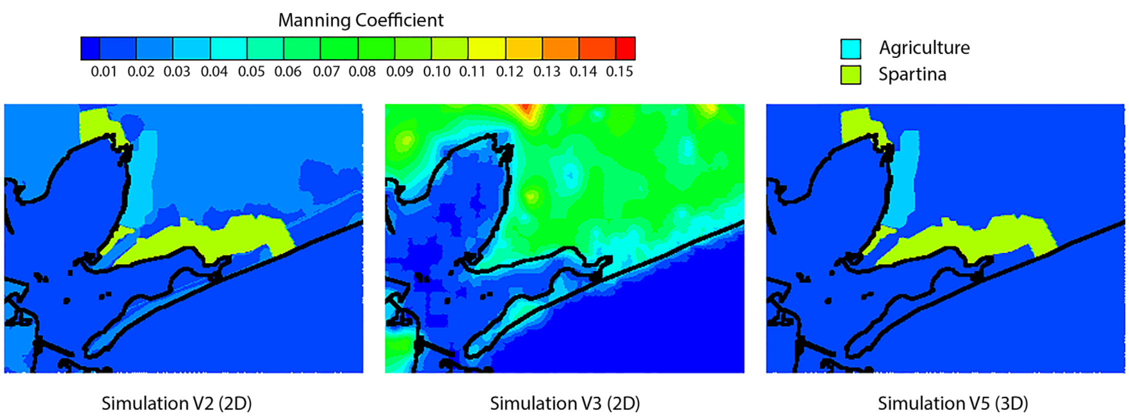

Figure 3. (a) Maps of Manning coefficients used for 2-D simulation V2; (b): Manning coefficients for 2-D simulation V3 extracted from *Hope et al.* [2013]; (c): vegetation conditions for 3-D simulation V5. 2-D simulation V1 uses a single constant Manning coefficient. 3-D simulation V4 has no vegetation. Morphologies are described within the text.

Modification to the continuity equation due to the presence of vegetation is unnecessary because even in dense canopies, vegetation only occupies less than 2% of each cell's volume [*Nepf and Vivoni*, 2000].

In these momentum equations, terms are introduced for including the effects of vegetation. C_f is the skin friction coefficient, C_p is the profile drag coefficient, A_f is the frontal area per unit volume, A_w is the wetted area per unit volume, and q is the square root of twice the turbulent kinetic energy. C_f is determined by

$$C_f = c_1 \left(\frac{\nu}{q\Lambda} \right)^{1/4} \tag{5}$$

Coupled to the momentum equation is a TKE equation:

$$\frac{\partial q^2}{\partial t} + u_k \frac{\partial q^2}{\partial u_k} = 2C_p (e^2+q^2)^{1/2} A_f e^2 - 2C_f A_w q^3 + 2A_v \left[\left(\frac{\partial u}{\partial z} \right)^2 + \left(\frac{\partial v}{\partial z} \right)^2 \right] + 0.3 \frac{\partial}{\partial z} \left(q\Lambda \frac{\partial q^2}{\partial z} \right) - \frac{q^3}{4\Lambda} \tag{6}$$

where the right-hand side contains a production term from frontal area, A_f, a dissipation term from wetted area, A_w, two shear production terms, and a turbulence dissipation term. $e = \sqrt{uu+vv+ww}$. The above equation allows turbulence to be generated at some point in the water column but transported to another location before becoming dissipated. It should be noted that the vegetation effects on flow and turbulence come from not only the stems, which are considered as cylinders providing profile drag, but also the leaves, which provide skin friction drag. According to equation (5), the effect of skin friction decreases for more turbulent flow, but the skin friction can be significant for very leafy vegetation such as mangroves and particularly relatively short mangroves which are mostly submerged in water and hence have large wetted area A_w for equations (1) and (2). The consequence of only including profile drag [*Temmerman et al*., 2007; *Hortsman et al*., 2013; *Zhao and Chen*, 2014; *Hu et al*., 2015] but not skin friction drag requires further investigation.

The turbulence macrolength scale, Λ, is a geometric constraint dependent upon distance from the free surface and vegetation densities. The constraints for Λ are [*Lewellen*, 1977; *Wilson and Shaw*, 1977; *Lewellen and Sheng*, 1980]:

$$\left| \frac{d\Lambda}{dz} \right| \le 0.65 \;\; and \;\; \Lambda \le \frac{\alpha}{C_p A_f} \tag{7}$$

$$\Lambda = 0 \;\; at \;\; z = 0 \tag{8}$$

where α is a model constant dependent upon canopy geometry. This vegetation model is described in detail by *LS14*, and is validated with the 3-D laboratory experiments of *Neumeier* [2007] and *Nepf and Vivoni* [2000]. Simulations here used values of $C_p = 0.2$, $c_1 = 0.125$, and $\alpha = 0.1$. These values are comparable to those found in validations using laboratory data in *LS14*. To resolve vegetation effects on waves, SWAN includes a vegetation model which modifies significant wave height, period, and direction based on the presence of vegetation [*Suzuki et al*., 2012]. This in turn affects radiation stress terms within the circulation model, but the influence of vegetation is not doubly counted.

We focus our investigation of the effects of vegetation on surge and inundation on Chambers County, Texas, where the most significant flooding during Ike occurred [*Hope et al*., 2013]. One main difference between 2-D and 3-D hydrodynamic model is the representation of bottom friction and roughness condition: 2-D model uses MC while 3-D model uses Zo. While Zo is consistent with the presence of a turbulent bottom boundary layer over a rough bottom, MC assumes complete mixing over the entire water column. In producing the results for V1, V2, V3, V4, and V5 in Table 2, no attempt was made to overly tune MC and Zo. V1 uses a constant MC and V4 uses a constant Zo and both gave reasonable overall model results throughout the model domain. MC for V1, 0.017, and Zo for V4, 0.05, are both a bit low for the CHA-003 and CHA-004 stations which are near vegetation. V2 uses a constant MC plus locally modified MC near vegetation. V3 uses a spatially varying MC field used by *Hope et al*. [2013]. Although additional tuning of MC or Zo could improve the simulated results, it was avoided because our goal is not to show that 2-D model can be continually tuned to give results similar to the 3-D results. Moreover, 2-D model cannot provide the vertical information that 3-D model produces.

Table 2. Simulations Conducted to Compare 2-D and 3-D Representations of Vegetation

Simulation	Dimensionality	Vegetation Effects Included
V1	2D	No
V2	2D	MC in Chambers County
V3	2D	ADCIRC MC map
V4	3D	No
V5	3D	VM in Chambers County

Figure 3 shows two different 2-D maps of MC and one 3-D map of vegetation which are used to compare the effects of vegetation. Figure 3a shows the 2-D MC map for simulation V2, with most cells having a MC of 0.017, agricultural cells having a MC of 0.03, and wetland vegetation having a MC of 0.1, both based on literature recommendation. Figure 3b shows a MC map for simulation V3, with the MC used by *Hope et al*. [2013] for Ike simulation. For the 3-D map shown in Figure 3c, cells within Chambers County are assigned vegetation data based upon their elevation, aerial photography, and hydrodynamic regime. Cells within the boundaries of a National Wildlife Refuges, or with aerial photography indicating similar plant morphologies are assigned a plant morphology akin to a *Spartina* marsh, and cells in areas used for agriculture are assigned a shorter plant morphology.

For the 3-D map (Figure 3c), it is necessary to quantify the amount of vegetation present in agricultural land and NWR land. Advancements in LIDAR technology are facilitating the development of high-resolution vegetation maps, including pictures of vertically varying vegetation density [*Nayegandhi et al*., 2005]. Although this is unavailable for the study region, reasonable assumptions can be made using aerial photography and ground-truthing images. The NWR land is mostly wetland vegetation, and much of it is tidally influenced *Spartina* [*Butcher*, 2003]. Because Hurricane Ike landed in September, it can be reasonably assumed that this vegetation was in full density and at least medium height, so cells within the NWR are assigned a vegetation height of 125 cm and stem density of 100 stems/m^2, both fairly typical for this ecosystem [*Webb and Newling*, 1985]. Agricultural land is mostly used for ranching, and is assigned a height of 25 cm, and a density of 100 stems/m^2. Both assumptions are proven useful and valid, although they could be improved with a comprehensive data set in the future.

To compare 2-D and 3-D representations of vegetation, five simulations are run, as listed in Table 2. All are 4 days in duration, with simulations over the entire storm period and including tides. Two are 3-D simulations, three are 2-D simulations, and one of the 3-D simulations includes the effects of vegetation, while two of the 2-D simulations include the vegetation effects. These simulations enable a detailed comparison of the two methods, which is essential to advance the science of storm surge modeling.

The USGS data set used to compare dimensionality was augmented to investigate the influence of vegetation. Of the 28 water levels used to compare simulations D1-D3, only two were located in Chambers County. If taken alone, these provide an insufficient picture of the effects of storm surge there. To augment these two stations, high water marks (HWMs) collected by FEMA within Chambers County [*Federal Emergency Management Agency*, 2010] are used to evaluate the quality of model results there. Consequently, each simulation result is evaluated for accuracy over the entire domain (with 41 data points) as well as within Chambers County alone (with 14 data points). These USGS and FEMA data will be made available to anyone who sends a request to the corresponding author, upon publication of this paper online. For each simulation, the maximum water level within each cell is recorded as the Envelope of High Water (EOHW). Maximum observed water levels are compared to those from the EOHW, which measures deviations of simulated results from the observed data.

2.4. Sediment Transport Modeling

Recent advances in observational geomorphology have identified marine sediment transport onto coastal wetlands as an important component of wetland stability [*Turner et al*., 2006]. This research has generated controversy [*Turner et al*., 2006; *Törnqvist et al*., 2007; *Turner et al*., 2007], and remarks have been made about the need for advancements in nearshore hydrodynamic modeling of sediment transport during storms [*Törnqvist et al*., 2007; *Turner et al*., 2007; *Williams*, 2010]. Hurricane Ike is a useful storm to explore this inquiry, because of its well-documented sediment deposition pattern [*Williams*, 2010, 2012; *Tweel and Turner* 2012]. In particular, *Tweel and Turner* [2012] noted that Hurricane Ike featured marine sediment deposition much further away from its landfall location than similar storms, such as Rita, Katrina, and Gustav.

Independently collected observations from both *Tweel and Turner* [2012] and *Williams* [2012] are combined here, and show that significant inland sediment deposition occurred over 150 km from where Ike made

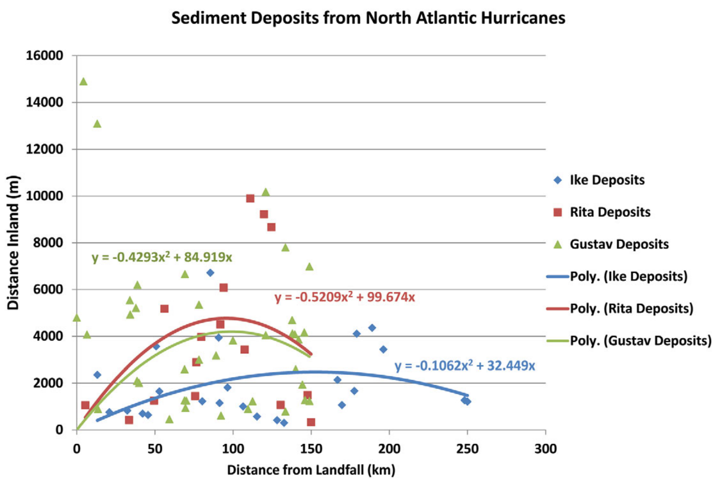

Figure 4. Inland sediment deposits from Hurricanes Rita, Gustav, and Ike. Data from *Williams* [2012] and *Tweel and Turner* [2012]. Note that this plot does not convey deposit thickness or total deposition by a storm.

landfall, which is anomalous when compared to Hurricanes Rita, Katrina, and Gustav. These data are shown in Figure 4, which show observations of inland sediment deposition for these four storms, and warrant our interest in the cause for sediment transport this far inland from the storm landfall location. The three colored polynomials represent the sediment deposition patterns inland during three storms. Clearly, during Ike, sediment deposition is spread over a wider coastal distance spanning 250 km from the landfall location while, during Rita and Gustav, sediment was spread over only a 150 km wide coast but further inland. To advance scientific understanding of the cause and likelihood for this kind of inland sediment deposition, this paper evaluates whether onshore marine sediment flux this (250 km) far from the hurricane landfall location during Ike is possible via 3-D modeling. The onshore sediment transport will be compared to the observed inland sediment deposition pattern shown in Figure 4. Again, detailed morphological modeling [e.g., *Coco et al*., 2014] is beyond the scope of this paper.

Sediment transport is modeled during Hurricane Ike simulation using a 1 s time step without including tides. The onshore sediment flux is calculated by multiplying the velocity and sediment concentration in the bottom-most layer. Three stations slightly offshore (OS1, OS2, and OS3, which are about 150, 200, and 250 km from the Ike landfall location, respectively) are selected, as shown in Figure 2. These stations are used to compare the capabilities of 2-D and 3-D models. As a proxy measurement for sediment transport, this is compared to velocity trajectories found in a 2-D model run using the same time step and duration. These two simulations are summarized in Table 3.

Sediment transport is included within CH3D-SSMS using a model developed by *Sheng et al*. [1993, 2002] and *Sheng and Kim* [2009], which includes mixing, resuspension, settling, deposition, and flocculation (for cohesive sediments). Bottom sediment erosion by currents and waves is described by the bed load transport formula developed by *van Rijn* [1984, 2007] and *Davies and Li* [1997] for noncohesive sediments and, for cohesive sediments, an erosion rate which depends on the bottom stress, bottom sediment property and vertical profile according to *Sheng et al*. [1993, 2002]. The model has been validated for wind-driven events in Lake Okeechobee, Tampa Bay, and Charlotte Harbor [e.g., *Sheng*, 1986; *Sheng et al*., 1993; *Chen and Sheng*, 2005; *Sheng and Kim*, 2009], and is shown to be able to simulate 3-D wind and wave-driven sediment transport. The model has been found to be particularly accurate for simulating high wind events during fronts and storms [*Sheng and Kim*, 2009], and complete model equations can be found in *Sheng* [1986], *Sheng et al*. [1993], and *Chen and Sheng* [2005]. The ability of 3-D storm surge models to simulate onshore transport of marine sediments represents a nontrivial scientific advancement in storm surge modeling, wetland ecology, and paleotempestology.

This sediment model's ability to accurately simulate deposition in coastal vegetation and/or the effects of vegetation on sediment deposition as outlined in *Sheng* [1986] is yet to be verified with comprehensive field data in the future. These processes are nonlinear and well-designed field experiments are needed to provide the comprehensive data for detailed model verification. In the simulations, sediment particles are assumed to be noncohesive with median diameter of 100 microns, bottom sediments are assumed to possess a critical stress for erosion on the order of 0.25 dyne/cm^2, using the bed load formula of *van Rijn* [1984, 2007], and a deposition

Table 3. Sediment Transport Simulations Conducted

Simulation	Dimensionality	Sediment Modeled
S1	3D	Yes
S2	2D	No

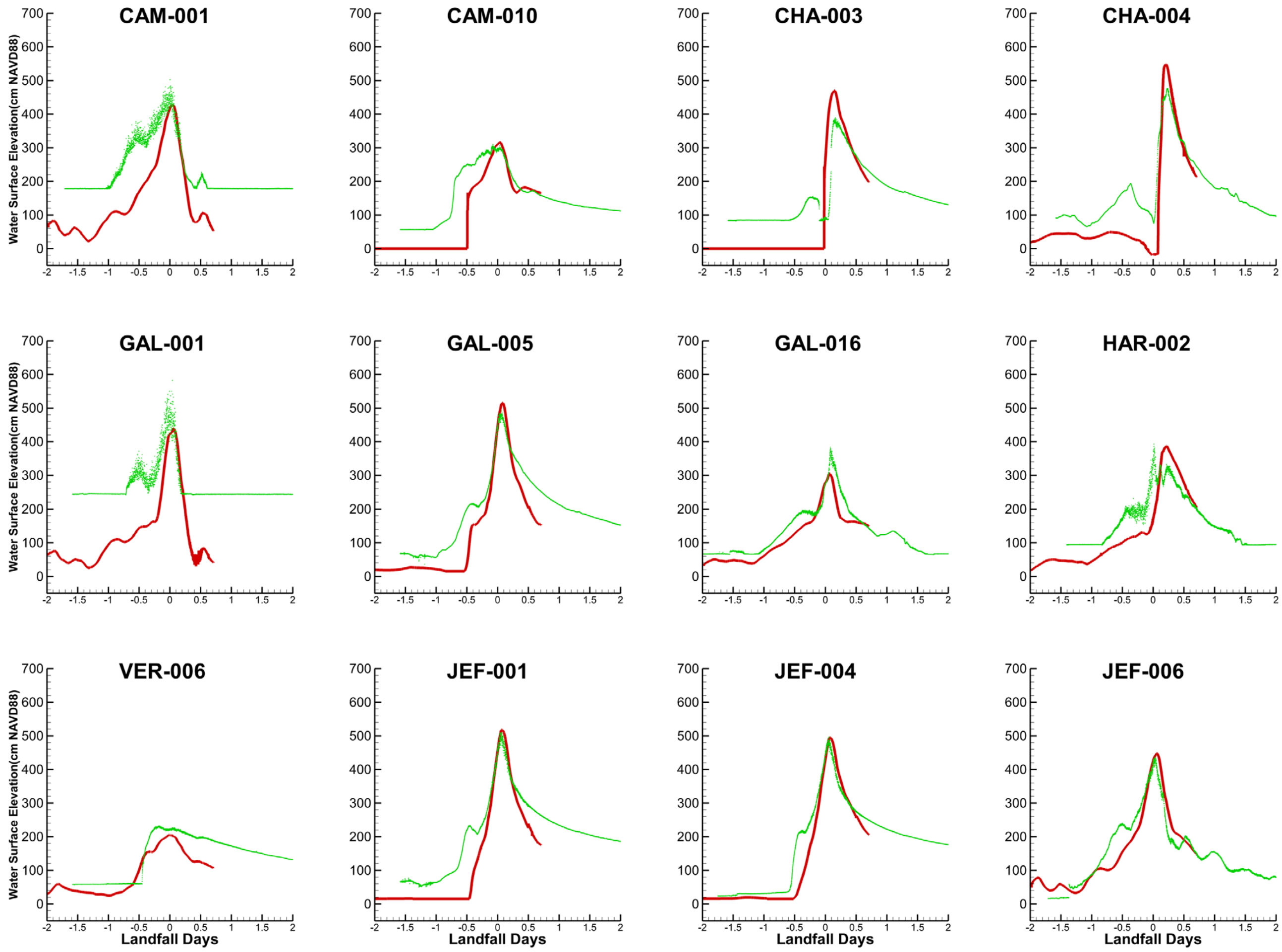

Figure 5. USGS data compared to modeled water level in Simulation D1. Modeled values in red, data in green.

velocity calculated following the formulas in *Sheng* [1986]. An initial suspended sediment concentration of 100 mg/L is assumed.

3. Results

3.1. 2-D Versus 3-D Comparison

To demonstrate the ability of the 3-D model to simulate the storm surge during Hurricane Ike, hydrographs for a set of the USGS data are compared to water levels from Simulation D1 in Figure 5. These hydrographs show the model is capable of simulating the forerunner, the increase in water level which occurred in the 12 h prior to the storm making landfall. At a few stations such as CAM-01 and GAL-01 which are near the shoreline, inaccurate topography, and error in wind field might have contributed to the initial error in surge. Nevertheless, the peak surges are generally well simulated by the 3-D model. While the 2-D results also show the forerunner, they are not as accurate as the 3-D results. A more quantitative comparison of the water levels simulated by D1–D3, as shown in Table 4, clearly reflects the higher accuracy of the 3-D results.

Figure 6 shows a comparison of the simulated and observed velocities at TABS Buoys R, B, and F for simulations D1–D3, and results from *Hope et al*. [2013]. Results from Simulation D1 include velocity in the bottom layer, velocity in the top layer, and vertically averaged velocity. Note that TABS buoys collect data roughly 2 m below sea level, and are unable to capture velocities over 1 m/s, so data are not present above this threshold velocity, or at the bottom or surface of the water column. This figure highlights the strong onshore

Table 4. Results From 2-D and 3-D Simulations of Hurricane Ike

Simulation	Dimensionality	Z_0 (3D) or MC (2D)	RMS Error for High Water Marks (cm)	Average Percent Error	Correlation Coefficient
D1	3D	0.05 cm	28.7 cm	6.1%	0.89
D2	2D	0.01	93.5 cm	22.9%	0.62
D3	2D	0.017	96.5 cm	25.0%	0.79

currents exceeding 1 m/s and significant vertical variation of horizontal currents during Ike, hence the need for measurement of vertical profiles of horizontal currents. The only available current observation could not measure currents above 1 m/s. Moreover, during the storm, there is significant movement of the free surface, making it difficult to discern the precise vertical location of the ADCP. As stated earlier, it is difficult to assess the accuracy of the vertically averaged velocity simulated by a 2-D model because it would require performing vertical averaging of observed vertical profile of horizontal velocities. The lack of observed vertical profile of velocities makes it difficult to assess the accuracy of the ADCIRC simulated vertically averaged velocity which deviates only slightly from the vertically averaged velocity from the 3-D model. The slight deviation between the ADCIRC velocity and the average velocity of the 3-D results could have resulted from differences in the model dimensionality, as well as other factors such as model domain/grid and forcing functions and other model parameters. No intention was made to reproduce the ADCIRC results because of the many differences (domain, grid, forcing, etc.) between their and our simulations and because it is not the focus of this paper. Nevertheless, it is safe to say that, when all other model factors are kept the same, 3-D models are more desirable because they contain more information and require less tuning.

3.2. Vegetation Effects on Surge

To quantitatively compare the effect of vegetation representations shown in Table 2, Table 5 contains data of average absolute error and percent deviations for the simulated and observed maximum water levels at the 41 data points at the USGS and FEMA stations. Fourteen data points are in the Chambers County. It is clear that V5 gives much better results than the others.

In addition to these statistics, time series for stations CHA-003 and CHA-004 are shown in Figure 7. It is clear that the vegetation-resolving model significantly reduced the simulation error at the 28 stations as well as the CHA-003 and CHA-004 stations near the vegetation. Increasing the vegetation density further reduces the error. However, it is not our interest here to tune the vegetation distribution. Instead, we believe further observation should include more water level data in vegetation area as well as more detailed vegetation data (including horizontal coverage, height, density, and vertically varying wetted area and frontal area) in the future in order to improve model accuracy. Because of interest in the ability of wetlands to reduce surge and water velocities, Figure 8 shows scatter plots of velocity and water level at stations CHA-003 and CHA-004 for simulations V4 and V5. This shows the significant reduction on horizontal flow velocity by vegetation when the 3-D model with VM is used.

3.3. Sediment Results

Onshore sediment flux is dependent upon velocity magnitude and direction, sediment concentration, and water depth. Plots of onshore sediment flux over the day of the storm are shown at stations OS1, OS2, and OS3 in Figure 9. Included are comparisons of onshore velocity in the bottom layer of the 3-D simulations

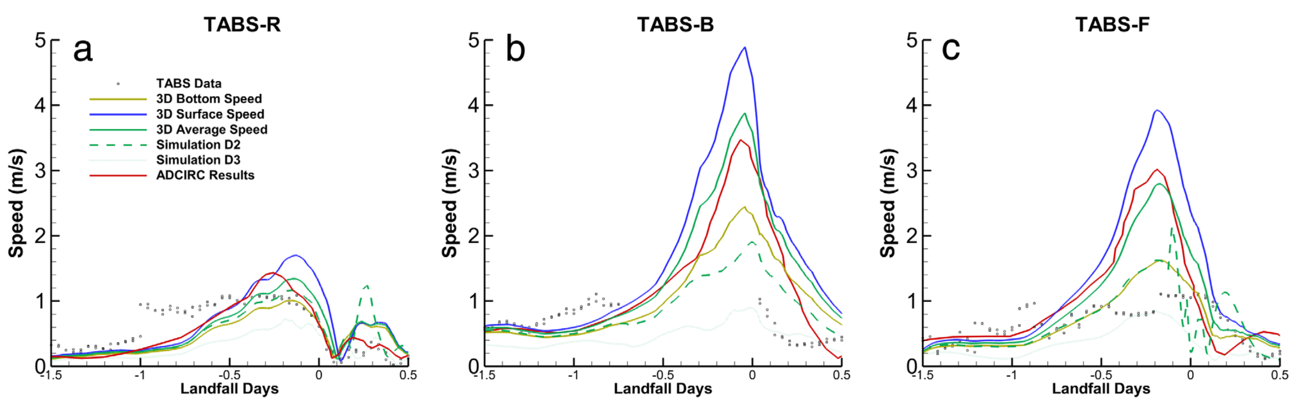

Figure 6. Simulated and measured onshore velocities at (a) TABS-R, (b) TABS-B, and (c) TABS-F Buoys during Hurricane Ike. Note that TABS Buoys measure velocities at 2 m below the surface but cannot measure velocities over 1 m/s.

Table 5. Summary of Deviations Between Simulated Water Level and FEMA HWMs for Hurricane Ike, Based on 41 Total Data Points

Simulation	Dimensionality	Vegetation Model	Average RMS Error (cm)	Average Percent Error
V1	2D	No	192.3	41.2%
V2	2D	MC	250.0	57.7%
V3	2D	MC	284.2	63.5%
V4	3D	No	123.4	25.1%
V5	3D	VM	84.9	14.1%

and the vertically averaged onshore velocity of the 2-D simulation. The near-bottom onshore current is strong and peaked to ~1 m/s at OS1 near the landfall location, but diminishes to a peak of 40 cm/s and 25 cm/s at the OS2 and OS3 stations further east from the landfall location, respectively. The corresponding near-bottom suspended sediment concentration at OS1, OS2, and OS3 peaked to 1600, 500, and 250 mg/L, respectively. These high sediment concentrations reflect significant sediment resuspension activity by the wave current-induced bottom stress. It is reasonable to expect that the significant onshore sediment fluxes at OS1, OS2, OS3 led to the significant inland sediment deposition pattern shown in Figure 4. Simulation of detailed morphological processes of inland sediment deposition, however, requires much more data which is unavailable and is beyond the scope of this paper.

4. Discussion

4.1. 2-D and 3-D Velocities

Figure 6 shows onshore velocity components at three TABS buoy stations prior to Hurricane Ike. There is remarkable agreement between the results prior to the storm, but during the storm, an impressive spread in current speeds exists. The 3-D simulation, as expected, has significantly different speeds at the top and bottom, up to 3.5 m/s. This implies 3-D models are important for proper modeling of sediment and pollutant transport during storm events, as well as many other density-dependent processes.

Additionally, as expected, 2-D current speeds are highly dependent upon the MC. This suggests that the MC can be manipulated for the purpose of increasing or reducing simulated velocities to match the observed ones. However, it should be noted that the MC was originally conceived as a means of describing 1-D flow in a pressure-driven channel dating back to 1867 [*Gauckler* 1867; *Manning* 1891; *Chow*, 1959], and was adopted by circulation modelers to simulate tidally driven flow in shallow estuaries [e.g., *Blumberg*, 1977]. It has been used in the simulation of storm surge events [*Bunya et al*., 2010; *Hope et al*., 2013], but some users have found the need to significantly adjust the canonical MC (e.g., doubling or halving the MC) to match the simulated and observed water levels and/or velocities [*Hope et al*., 2013]. However, performing excessive tuning of MC to improve agreement between simulated and observed water levels defeats the purpose of modeling and particularly forecasting. Given the significant difference in vertically varying velocities shown here, the importance of the geophysics of storm surge events, and the relative dearth of velocity data in the open coastal water, it is clear that there is a major scientific need for more velocity data in the open coastal water during storms. For simplicity, tides were excluded from the sediment transport

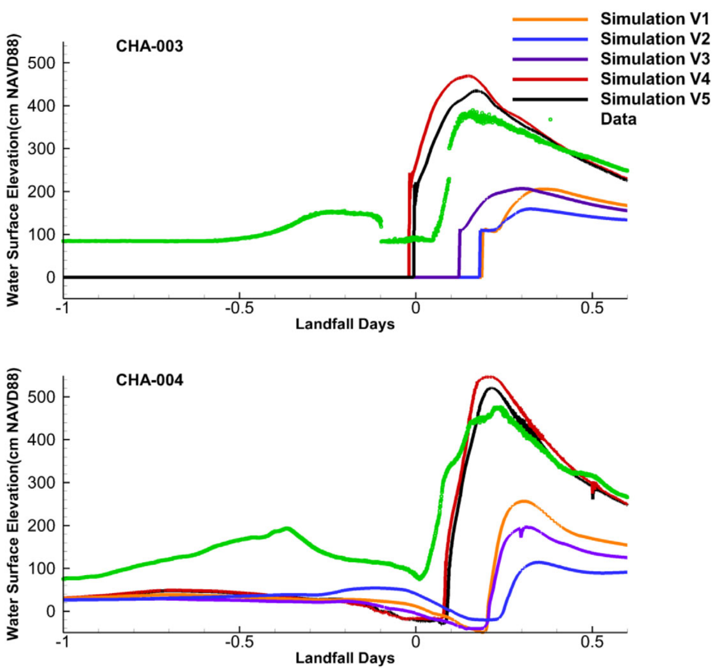

Figure 7. Water levels at stations CHA-003 and CHA-004.

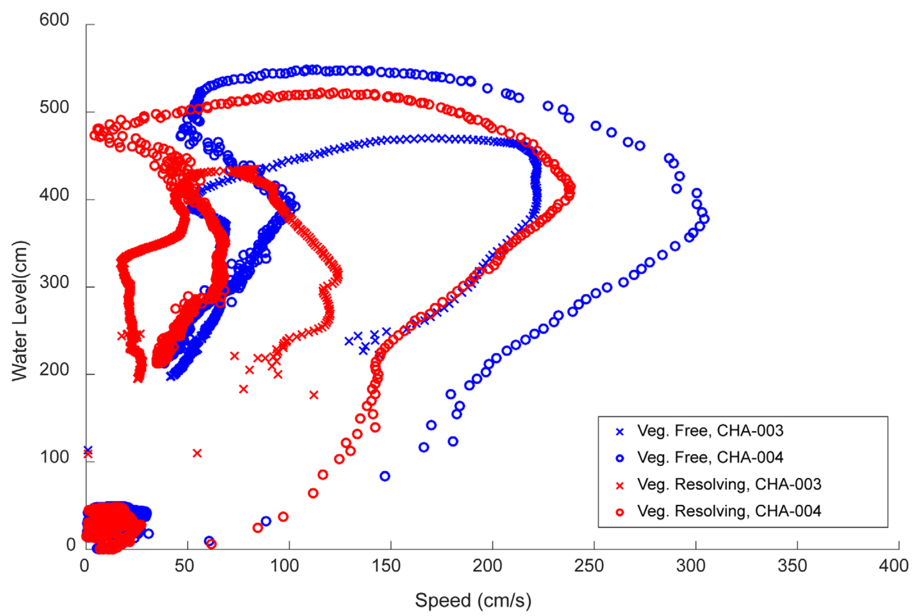

Figure 8. Scatter plots of speed and velocity for simulations V4 and V5 at USGS stations CHA-003 and CHA-004.

simulations. However, since tides only add an oscillatory onshore-offshore current, that should not significantly alter the onshore sediment transport due to surge and wave.

4.2. Vegetation Representation

A major advancement shown in this paper is the ability of a 3-D model to simulate the effects of vegetation during a real storm. The 2-D and 3-D time series of water level in Chambers County as seen in Figure 7 are very different. The 3-D simulations V4 and V5 produce quite accurate water level in vegetated area, particularly when a 3-D vegetation map is included for Simulation V5. 3-D simulations also contain more information about vertical velocity gradients, energy dissipation, and the physical processes of flow through vegetation in 3-D.

2-D water levels in Chambers County from Simulations V1–V3 are generally lower than the observed values, indicating that the ADCIRC MC map does not produce reasonable water levels, whereas the 3-D vegetation map improves results in Chambers County. This suggests that the MC is not a robust and interoperable characterization of bottom roughness, or momentum lost to vegetation and the bottom surface, and should be used with caution.

4.3. Sediment Transport

A significant process highly dependent upon bottom currents is sediment transport. The results shown in Figure 9 contain several novel insights. The significant onshore sediment fluxes from 3-D simulations of the storm indicate that hydrodynamically, onshore sediment transport during a hurricane is realistic, reinforcing the findings of *Turner et al*. [2006]. Second, the sediment fluxes at these stations, which are (150, 200, 250) km away from where the storm made landfall, corresponds well with the onshore sediment deposition pattern observed by *Williams* [2012] and *Tweel and Turner* [2012] as shown in Figure 4. During Rita, however, there was little inland sediment deposition because onshore sediment fluxes at these locations were negligible due to the lack of strong onshore currents and sediment resuspension. It should be noted that the onshore transport and deposition of marine sediments during storms by surge and wave-induced currents have not been successfully simulated before, and Ike's unique onshore sediment deposition pattern was unexplained until now.

While the good correlation between the observed sediment deposition and simulated onshore sediment flux is quite encouraging, the scarcity of detailed data does not permit a full blown verification of the 3-D sediment transport simulation. Nevertheless, our results showed that it is most likely that the deposited sediments on land originated from onshore transport of resuspension and transport of offshore sediments

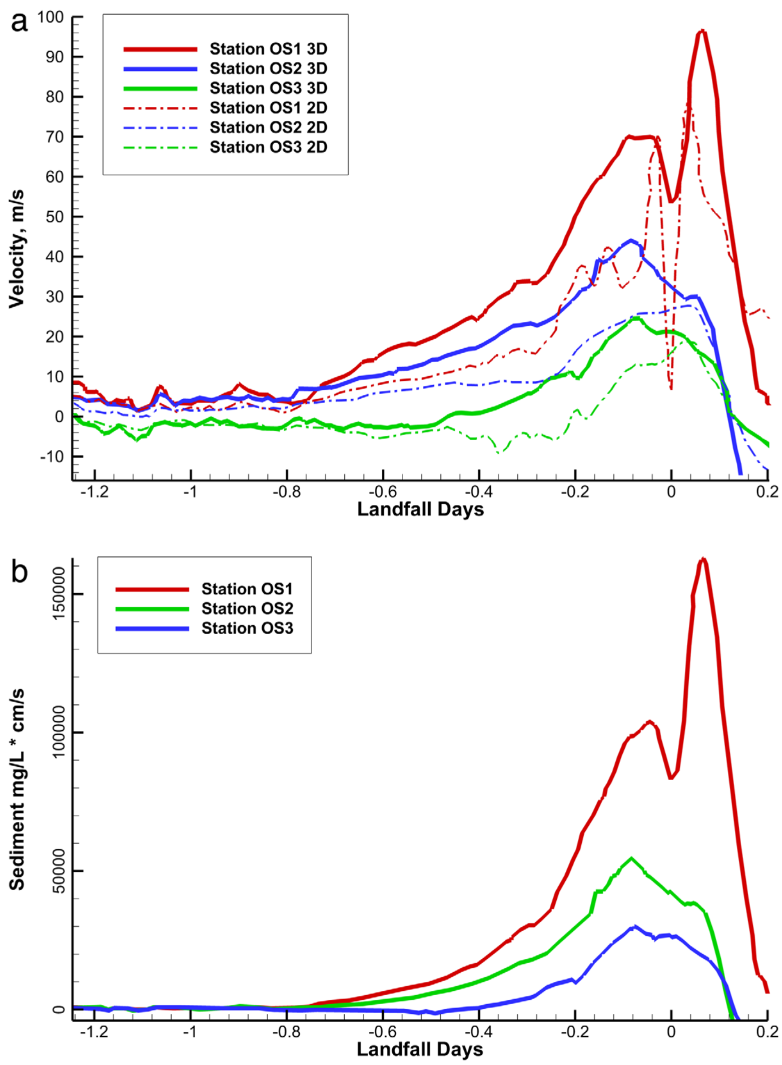

Figure 9. Simulated onshore velocities (a) and onshore sediment flux (b) for Hurricane Ike. 3-D velocities are in the bottom layer, 2-D velocities are in the middle of the water column. These significant onshore sediment fluxes correspond well with the inland sediment deposition patterns shown in Figure 4.

by the wave-surge induced onshore currents simulated by the CH3D-SWAN model. Further investigation of this requires a more comprehensive modeling and observing study in the future.

Comparing the 2-D onshore velocity components with those of the bottom layer in the 3-D simulations points to the value of 3-D models in simulating the complex 3-D dynamics of storm surge. During the day preceding Ike, high shore-parallel winds caused the buildup of a water anomaly which became the forerunner [*Kennedy et al*., 2011; *Hope et al*., 2013]. However, these shore parallel winds had hydrodynamic effects which extend to the bottom of the water column. As one descends in the water column, the relative importance of wind effects decrease while the relative importance of Coriolis effects increase, and consequently, the onshore velocity component of a 3-D velocity is greater than that of the 2-D vertically averaged velocity. Without simulating the storm in 3-D, the significant onshore velocity at Station OS3 (and sediment resuspension) would not be captured, as well the sediment deposited far inland from the storm center.

In a 3-D sediment transport model, various processes such as transport, settling, deposition, and resuspension are based on 3-D hydrodynamic processes induced by waves and currents which are simulated by dynamically coupled CH3D-SWAN. Sediment deposition and resuspension depend on wave-current interaction inside the bottom boundary layer. Because of the significant vertical variation of the horizontal currents, it is more appropriate to use the bottom layer sediment transport, instead of the vertically averaged sediment transport, as the surrogate for the onshore sediment flux. Using a 2-D sediment transport model would require much more calibration with field data, including currents and sediment data, hence it is not attempted.

5. Conclusions

The simulations and results described in this paper show advancement in scientific understanding of complex storm surge dynamics during a real hurricane. In particular, they show the importance of 3-D simulations for accurate prediction of velocities in the open coastal water, the effects of vegetation on surge, and onshore sediment transport. Scientists attempting to improve the hydrodynamic modeling of storm surge should consider incorporating these effects into their models, because status-quo 2-D models using the MC approach cannot accurately simulate these processes. Using a spatially varying MC field, the 2-D model results are still not as accurate as the 3-D model results. In fact, according to the study of *LS14*, MC is a function of bottom roughness as well as the flow condition. Therefore, a temporally and spatially varying MC maybe needed to significantly improve the 2-D model results, which would make the 2-D modeling much more cumbersome and less robust.

Vertical variability in horizontal coastal currents during a storm is significant, even in the relatively shallow coastal waters of the Gulf of Mexico, and this has consequences for hydrodynamics, sediment and pollutant transport, and turbulent mixing. With abundant concerns related to oil settled on the bottom of the Gulf, 3-D modeling efforts are needed to evaluate the potential for transport of this settled oil onshore during a storm [*Liu and Sheng*, 2014].

Federal, state, and local governments are considering the use of coastal vegetation as a means of reducing the risk of storm surge. Properly approaching the implementation of these projects requires modeling efforts, and this paper demonstrates that 3-D representations of the effects of vegetation in real storms are more robust than 2-D representations, and they lead to much more accurate results. The 3-D vegetation resolving models can be used for quantitative assessment of the values of ecological service provided by coastal wetlands [*Barbier et al*., 2011; *Costanza et al*., 1997; *Duarte et al*., 2013] and to improve the estimates obtained by empirical methods.

Recent research has found that sediment transport onshore during hurricanes plays a crucial role in the formation of landscapes. This process has not been previously simulated, and this paper represents a step forward in confirming this finding. Additionally, this paper shows a 3-D model produces significantly more onshore momentum and sediment transport than a 2-D model. While this is encouraging, further study is needed to further elucidate all the processes involved in the deposition of marine sediments on land. An integrated surge-vegetation-sediment model with a comprehensive observing effort is needed to simulate the complex processes in a rapidly changing coastline due to more frequent storms and sea level rise.

Accurate simulation of complex 3-D processes in coastal environment requires the use of accurate data (winds, tides, bathymetry, topography) and appropriate model features (model domain, horizontal and vertical grid, wave-induced radiation stress, wave-current boundary layer, and sediment transport processes such as deposition, resuspension, and stratification). While it may be possible to parameterize all the 3-D processes into a 2-D model and use it to achieve results that are comparable to the vertically averaged results of 3-D model, it is not the purpose of this paper here. This paper showed that, by keeping everything else in a model simulation the same, 3-D models generally give more reliable and detailed information with less tuning than 2-D models. This statement should apply to other 3-D models such as ROMS [*Shchpetkin and McWilliams*, 2005] and Delft3D [*Hortsman et al*., 2013; *Hu et al*., 2015].

Last but not least, this study points out the need for more detailed observation data of water level and currents, vegetation, and sediment transport in coastal waters, and particularly in the vegetation zone, for enhancing the understanding and modeling of complex 3-D storm surge dynamics.

Acknowledgments
This study is supported by the University of Florida, Florida Sea Grant Project R/C-S-55, the U.S. IOOS Program Project IOOS.11(033), and the National Oceanic and Atmospheric Administration National Climate Services Project #NA11OAR4310105. The authors will abide by the JGR data policy. Request for the USGS and FEMA water level data used in the paper should be sent to the corresponding author (pete@coastal.ufl.edu) upon publication of the paper online. The authors would like to thank the insightful comments of two anonymous reviewers.

References

Barbier, E. B., S. D. Hacker, C. Kennedy, E. W. Koch, A. C. Stier, and B. R. Silliman (2011), The value of estuarine and coastal ecosystem services, *Ecol. Monogr.*, *81*, 169–193.

Bode, L., and T. A. Hardy (1997), Progress and Recent Developments in Storm Surge Modeling, *J. Hydraulic Eng.*, *123*, doi:10.1061/(ASCE)07339429(1997)123:4(315).

Booij, R., C. Ris, and H. Holthuijsen (1999), A third-generation wave model for coastal regions: 1. Model description and validation, *J. Geophys. Res.*, *104*, 7649–7666, doi:10.1029/98JC02622.

Blumberg, Alan F. (1977), Numerical Tidal Model of Chesapeake Bay, *J. Hydralics Div.*, 12661–12671.

Bunya, S., et al. (2010), A high-resolution coupled riverine flow, tide, wind, wind wave, and storm surge model for southern Louisiana and Mississippi. Part I: Model development and validation, *Mon. Weather Rev.*, *138*, 345–377.

Butcher, R. D. (2003), *America's National Wildlife Refuges: A Complete Guide*, Roberts Rinhart Publ., 512 pp.

Chen, X., and Y. P. Sheng (2005), Three-dimensional modeling of sediment and phosphorus dynamics in Lake Okeechobee, Florida: Spring 1989 simulation, *J. Environ. Eng.*, *131*, 359–374.

Chow, V. T. (1959), *Open Channel Hydraulics*, McGraw-Hill, N. Y.

Coco, G., N. Senechal, A. Rejas, K. R. Bryan, S. Capo, J. P. Parisot, J. A. Brown, and J. H. M. MacMahan (2014), Beach response to a sequence of extreme storms, *Geomorphology*, *204*, 493–501.

Condon, A., and Y. P. Sheng (2012), Evaluation of coastal inundation hazard for present and future climates, *Nat. Hazards*, doi:10.1007/s11069-011-9996-0.

Condon, A. J., Y. P. Sheng, and V. A. Paramygin (2013), Toward high-resolution, rapid, and probabilistic forecasting of the inundation threat of landfalling hurricanes, *Mon. Weather Rev.*, *141*, doi:10.1175/MWR-D-12-00149.1.

Costanza, R., et al. (1997), The value of the world's ecosystem services and natural capital, *Nature*, *387*, 253–260.

Davies, A. G., and Z. Li (1997), Modeling sediment transport beneath regular symmetrical and asymmetrical waves above a plane bed, *Cont. Shelf Res.*, *17*(5), 555–582.

Davis, J. R., V. A. Paramygin, D. Forrest, and Y. P. Sheng (2010), Toward the probabilistic simulation of storm surge and inundation in a limited-resource environment, *Mon. Weather Rev.*, *138*, 2953–2974, doi:10.1175/2010MWR3136.1.

Duarte, C. M., I. J. Losada, I. E. Hendriks, I. Mazarrasa, and N. Marba (2013), The role of coastal plant communities for climate change mitigation and adaptation, *Nat. Clim. Change*, doi:10.1038/NCLIMATE1970.

Federal Emergency Management Agency (2010), *Hurricane Ike in Texas and Louisiana: Mitigation Assessment Team Report*.

Ferreiera, C. M., J. L. Irish, and F. Olivera (2014), Uncertainty in hurricane surge simulation due to land cover specification, *J. Geophys. Res. Oceans*, *119*, 1812–1827, doi:10.1002/2013JC009604.

Gauckler, P. (1867), *Etudes Théoriques et Pratiques sur l'Ecoulement et le Mouvement des Eaux, Comptes Rendues de l'Académie des Sciences*, pp. 818–822, Paris, France, Tome 64.

Grant, W. D., and O. S. Madsen (1979), Combined wave and current interaction with a rough bottom, *J. Geophys. Res.*, *84*, 1797–1808, doi:10.1029/JC084iC04p01797.

Hope, M. E., et al. (2013), Hindcast and validation of Hurricane Ike (2008) waves, forerunner, and storm surge, *J. Geophys. Res. Oceans*, *118*, 4424–4460, doi:10.1002/jgrc.20314.

Horstman, E. M., C. M. Dohmen-Janssen, and S. J. M. H. Hulscher (2013), Modeling tidal dynamics in a mangrove creek catchment in Delft3D, in *Coastal Dynamics 2013*, edited by P. Bonneton and T. Garlan, pp. 833–844, Arcachon, France.

Hu, K., Q. Chen, and H. Wang (2015), A numerical study of vegetation impact on reducing storm surge by wetlands in a semi-enclosed estuary, *Coastal Eng.*, *95*, 66–76.

Jelesnianski, C. P., J. Chen, and W. A. Shaffer (1992), SLOSH: Sea, lake, and overland surges from hurricanes, *NOAA Tech. Rep. NWS 48*, Silver Springs, Md.

Kennedy, A. B., et al. (2011), The origin of the Hurricane Ike forerunner, *Geophys. Res. Lett.*, *11*, L08608, doi:10.1029/2011GL047090.

Kerr, P. C., et al. (2013a). U.S. IOOS coastal and ocean modeling testbed: Inter-model evaluation of tides, waves, and hurricane surge in the Gulf of Mexico, *J. Geophys. Res. Oceans*, *118*, 5129–5172, doi:10.1002/jgrc.20376.

Kerr, P. C., R. C. Martyr, A. S. Donahue, M. E. Hope, J. J. Westerink, R. A. Luettich Jr., A. B. Kennedy, J. C. Dietrich, C. Dawson, and H. J. Westerink (2013b), U.S. IOOS coastal and ocean modeling testbed: Evaluation of tide, wave, and hurricane surge response sensitivities to mesh resolution and friction in the Gulf of Mexico, *J. Geophys. Res. Oceans*, *118*, 4633–4661, doi:10.1002/jgrc.20305.

Kumar, N., G. Voulgaris, and J. C. Warner (2011), Implementation and modification of a three-dimensional radiation stress formulation for surf zone and rip current applications, *Coastal Eng.*, *58*, 1097–1117.

Lapetina, A., and Y. P. Sheng (2014), Three-dimensional modeling of the effects of coastal vegetation on storm surge and inundation, under review, *Estuaries Coasts*, doi:10.1007/s12237-013-9730-0, in press.

Lewellen, W. S. (1977), The use of invariant modeling, in *Handbook of Turbulence*.

Lewellen, W. S., and Y. P. Sheng (1980), *Modeling of Dry Deposition of SO2 and Sulfate Aerosols*, Aeronaut. Res. Assoc. -Princeton, Princeton, N. J.

Liu, T., and Y. P. Sheng (2014), Three dimensional simulation of transport and fate of oil spill under wave induced circulation, *Mar. Pollut. Bull.*, *80*, 148–159.

Liu, H., K. Zhang, Y. Li, and L. Xie (2013), Numerical study of the sensitivity of mangroves in reducing storm surge and flooding to hurricane characteristics in southern Florida, *Cont. Shelf Res.*, 51–65, doi:10.1016/j.csr.2013.05.015.

Loder, N., J. Irish, M. Cialone, and T. Wamsley (2009), Sensitivity of hurricane surge to morphological parameters of coastal wetlands, *Estuarine Coastal Shelf Sci.*, 625–636, doi:10.1016/j.ecss.2009.07.036.

Luettich, R., J. J. Westerink, and N. W. Scheffner (1992), ADCIRC: an advanced three-dimensional circulation model for shelves coasts and estuaries, report 1: theory and methodology of ADCIRC-2DDI and ADCIRC-3DL. DRP-92-6, U.S. Army Engineers Waterways Experiment Station, 137 pp., Vicksburg, Mass.

Manning, R. (1891), On the flow of water in open channels and pipes, *Trans. Inst. Civ. Eng. Ireland*, *20*, 161–207.

Nayegandhi, A., J. C. Brock, and C. W. Wright (2005), Classifying Vegetation Using NASA's Experimental Advanced Airborne Research LIDAR (EAARL) at Assateague Island National Seashore, paper presented at ASPRS 2005 Annual Conference, Baltimore, Md.

Nepf, H., and E. Vivoni (2000), Flow structure in depth-limited, vegetated flow, *J. Geophys. Res.*, *105*, 28,547–28,557, doi:10.1029/2000JC900145.

Neumeier, U. (2007), Velocity and turbulence variations at the edge of saltmarshes, *Cont. Shelf Res.*, 1046–1059, doi:10.1016/j.csr.2005.07.009.

Powell, M. D., S. H. Houston, L. R. Amat, and N. Morisseau-Leroy (1998), The HRD real-time hurricane wind analysis system, *J. Wind Eng. Ind. Aerodyn.*, 53–64, doi:10.1016/S0167-6105(98)00131-7.

Rego, J., and C. Li (2010), Storm surge propagation in Galveston Bay during Hurricane Ike, *J. Mar. Syst.*, *82*, 265–279, doi:10.1016/j.jmarsys.2010.06.001.

Resio, D., and J. J. Westerink (2008), Modeling the physics of storm surges, *Phys. Today*, 33–38, doi:10.1063/1.2982120.

Shchpetkin, A. F., and J. C. McWilliams (2005), The regional ocean modeling system, *Ocean Model*, *9*, 347–404.

Sheng, Y. P. (1986), Modeling bottom boundary layer and cohesive sediment dynamics in coastal and estuarine waters, in *Estuarine Cohesive Sediment Dynamics*, edited by A. J. Mehta, vol. 14, pp. 351–400, Springer, N. Y.

Sheng, Y. P., and T. Kim (2009), Skill assessment of an integrated modeling system for shallow coastal and estuarine ecosystems, *J. Mar. Syst.*, *76*(1–2), 212–243.

Sheng, Y. P., and T. Liu (2011), Three-dimensional simulation of wave-induced circulation: Comparison of three radiation stress formulations, *J. Geophys. Res.*, *116, C05021*, doi:10.1029/2010JC006765.

Sheng, Y. P., and C. Villaret (1989), Modeling the effect of suspended sediment stratification on bottom exchange processes, *J. Geophys. Res.*, *94*, 14,429–14,444, doi:10.1029/JC094iC10p14429.

Sheng, Y. P., D. Eliason, and X. Chen (1993), SED3D, A Three-Dimensional Numerical Model of Hydrodynamics and Sediment Transport in Lakes and Estuaries: Theory, Model Development, and Documentation, 326 pp., U.S. Environ. Prot. Agency, Off. Res. and Dev., Environ. Res. Lab., Athens, Ga.

Sheng, Y. P., J. R. Davis, D. Sun, C. Qiu, K. J. Park, T. Kim, and Y. Zhang (2002), Application of an integrated modeling system of estuarine and coastal ecosystem to Indian River Lagoon, Florida, in *7th International Conference on Estuarine and Coastal Modeling*, edited by M. Spaulding, pp. 329–343, Am. Soc. of Civ. Eng.

Sheng, Y. P., V. Alymov, and V. Paramygin (2010a), Simulation of storm surge, wave, current, and inundation in the Outer Banks and Chesapeake Bay during Hurricane Isabel in 2003: The importance of waves, *J. Geophys. Res.*, *115*, C04008, doi:10.1029/2009JC005402.

Sheng, Y. P., Y. Zhang, and V.A. Paramygin (2010b), Simulation of storm surge, wave, and coastal inundation in the Northeastern Gulf of Mexico region during Hurricane Ivan in 2004, *Ocean Modell.*, *35*(4), 314–331, doi:10.1016/j.ocemod.2010.09.004.

Sheng, Y. P., A. J. Lapetina, and G. Ma (2012), The reduction of storm surge by vegetation canopies: Three-dimensional Simulations, *Geophys. Res. Lett.*, *39*, L20601, doi:10.1029/2012GL053577.

Smagorinsky, J. (1964), Implications of dynamical modelling of the general circulation on long-range forecasting, in *WMO-IUGG Symposium on Research and Development Aspects of Long-range Forecasting, WMO Tech. Note 62*, pp. 131–137, Boulder, Colo.

Suzuki, T., M. Zijlema, B. Burger, M. C. Meijer, and S. Narayan (2012), Wave dissipation by vegetation with layer schematization in SWAN, *Coastal Eng.*, 64–71, doi:10.1016/j.coastaleng.2011.07.006.

Temmerman, S., T. J. Bouma, J. van de Koppel, D. van der Wal, M. B. de Vries, and P. M. J. Herman (2007), Vegetation causes channel erosion in a tidal landscape, *Geology*, *35*(7), 631–634.

Tennekes, H., and J. Lumley (1972), *A First Course in Turbulence*, 320 pp., MIT Press.

Törnqvist, T. E., C. Paola, G. Parker, K. Liu, D. Mohrig, J. M. Holbrook, and R. R. Twilley (2007), Comment on ''Wetland Sedimentation from Hurricanes Katrina and Rita,'' *Science*, *316*, doi:10.1126/science.1136780.

Turner, R. E., J. J. Baustian, E. M. Swenson, and J. S. Spicer (2006), Wetland sedimentation from hurricanes Katrina and Rita, *Science*, *314*, doi:10.1126/science.1129116.

Turner, R. E., J. J. Baustian, E. M. Swenson, and J. S. Spicer (2007), Response to comment on ''Wetland Sedimentation from Hurricanes Katrina and Rita,'' *Science*, *316*, doi:10.1126/science.1136869.

Tutak, B., and Y. P. Sheng (2011), Effect of tropical cyclones on residual circulation and momentum balance in a subtropical estuary and inlet: Observation and simulation, *J. Geophys. Res.*, *116*, C06014, doi:10.1029/2011JC006988.

Tweel, A. W., and R. E. Turner (2012), Landscape-scale analysis of wetland sediment deposition from four tropical cyclone events, *PLOS One*, doi:10.1371/journal.pone.0050528.

van Rijn, L. C. (2007), Unified view of sediment transport by currents and waves. I: Initiation of motion, bed roughness, and bed-load transport, *J. Hydraul. Eng.*, *133*(6), 649–667.

Wamsley, T. V., M. A. Cialone, J. M. Smith, J. H. Atkinson, and J. D. Rosati (2010), The potential of wetlands in reducing storm surge, *Ocean Engineering*, *37*, 59–68.

Weaver, R. J., and R. A. Luettich (2009), 2D vs. 3D storm surge sensitivity in ADCIRC: Case study of hurricane isabel, in *Proceedings of the 11th International Conference of Estuarine and Coastal Modeling*, pp. 762–779, Am. Soc. Civ. Eng., Seattle, Wash.

Webb, J. W., and C. J. Newling (1985), Comparison of natural and man-made salt marshes in galveston bay complex, Texas, *Wetlands*, *4*, doi:10.1007/BF03160488.

Weisberg, R., and L. Zheng (2008), Hurricane storm surge simulations comparing three-dimensional with two-dimensional formulations based on an Ivan-like storm over the Tampa Bay, Florida region, *J. Geophys. Res.*, *113*, C12001, doi:10.1029/2008JC005115.

Williams, H. F. (2010), Storm surge deposition by hurricane Ike on the McFaddin National Wildlife Refuge, Texas: Implications for paleotempestology studies, *J. Foraminiferal Res.*, 210–219, doi:10.2113/gsjfr.40.3.210.

Williams, H. F. (2012), Magnitude of Hurricane Ike storm surge sedimentation: Implications for coastal marsh aggradation, *Lett. Earth Surf. Processes Landforms*, *37*, doi:10.1002/esp.3252.

Wilson, N. R., and R. Shaw (1977), A higher order closure model for canopy flow, *J. Appl. Meteorol.*, *16*, 1197–1205, doi:10.1175/1520-0450(1977)016.

Zhang, K., H. Liu, Y. Li, H. Xu, J. Shen, and J. Rhome (2012), The role of mangroves in attenuating storm surges, *Estuarine Coastal Shelf Sci.*, *102–103*, 11–23, doi:10.1016/j.ecss.2012.02.021.

Zhao, H., and Q. Chen (2014), Modeling attenuation of storm surge over deformable vegetation: Methodology and verification, *J. Eng. Mech.*, 140.